Isomerization of Carotenoids in the Presence of MCM-41 Molecular Sieves: EPR and HPLC Studies

Yunlong Gao, Lowell D. Kispert,* Tatyana A. Konovalova, and Jesse N. Lawrence

Department of Chemistry, BOX 870336, University of Alabama, Tuscaloosa, Alabama 35487-0336

Received: July 17, 2003; In Final Form: March 26, 2004

Isomerization of all-trans β-carotene and canthaxanthin embedded in solid MCM-41 and Ti−MCM-41 occurs during photoirradiation. The isomerization proceeds with high efficiency, primarily via the carotenoid radical cation ($Car^{\bullet+}$). The intermediacy of $Car^{\bullet+}$ was confirmed by studies of the isomerization caused by oxidation of these two compounds in Fe−MCM-41. Strong selective formation of the 13-cis isomer occurs for all-trans β-carotene, but no such selectivity was found for canthaxanthin. These phenomena are attributed to different orientations of the two compounds in these hosts. Molecular mechanics calculations show that formation of the 13-cis isomer of β-carotene is more favorable than that of other cis isomers in the MCM-41 host.

Introduction

Carotenoids (Car) are known to have two major functions in photosystems: light-harvesting and photoprotection. There are several stereoisomers of Car in photosystems. Scheme 1 shows commonly observed isomers of β-carotene (**I**) and canthaxanthin (**II**). The all-trans conformation of carotenoids is selected by the light-harvesting complexes, whereas the 15-cis conformation of carotenoids is selected by the reaction centers (RCs).[1] What is the reason for the natural selection of the 15-cis geometry by the RCs? Two explanations[1] have been proposed: one is that 15-cis Car was bound, by chance, to an ancestor RC and was then inherited by the RCs of photosynthetic organisms. The other is that the 15-cis arrangement is chosen by the RCs because of a functional advantage under the physiological conditions in the plant. To date, neither of these explanations has been considered to be the correct interpretation.

Photoisomerization of Car can be achieved via the lowest-lying triplet (T_1) state.[2] For example,[2] the quantum yield (the amount of isomerization per T_1 species generated) from all-trans **I** to cis species is 0.004, and the quantum yields from cis species of β-carotene to all-trans β-carotene are 7-cis, 0.12; 9-cis, 0.15; 13-cis, 0.82; and 15-cis, 0.98. Given such low quantum yields from all-trans to cis and high quantum yields from cis to all-trans, another question arises: how does the high cis/trans ratio of Car occur in RCs? For example,[3] 15-cis is the major component of β-carotene in the photosystem II RC of spinach. Some years ago the formation and accumulation of β-carotene radical cation ($Car^{\bullet+}$) in the photosystem II reaction center was detected. The process is induced by photooxidized chlorophyll, $P680^{\bullet+}$ (Car donates an electron to $P680^{\bullet+}$).[4−6] The $Car^{\bullet+}$ can be reduced by electron donation from a monomeric chlorophyll and also by cytochrome b_{559}.[7] Previous studies[8−10] by our group showed that isomerization of Car readily occurs via $Car^{\bullet+}$ or Car^{2+}. AM 1 calculations[8] of the energy barriers of geometric transformation via $Car^{\bullet+}$ or Car^{2+} support this result.

Does the environment of Car affect the selectivity of isomerization of Car? Is the high cis/trans ratio of Car in the RCs due to isomerization via $Car^{\bullet+}$? These questions were the impetus for the present study.

SCHEME 1. Structures of Isomers of Carotenoids

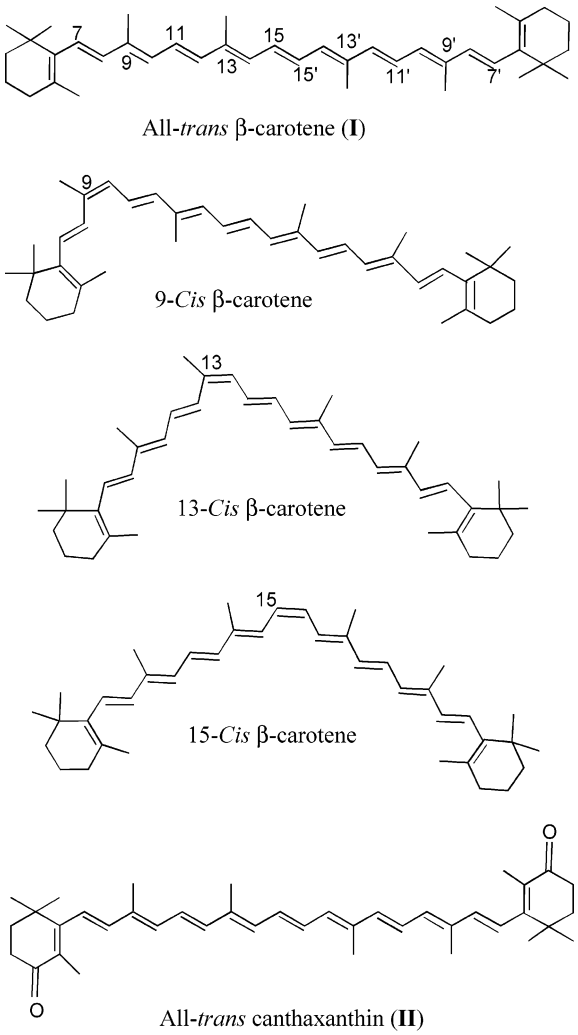

Previous studies[8−12] on the isomerization of Car, carried out in various solvents, provided an environment that is totally different from the rigid protein environment of RCs. Recently, a HYSCORE study[13] of $Car^{\bullet+}$ formed by oxidation of Car on

* Corresponding author.

10.1021/jp036091e CCC: $27.50
Published on Web 04/20/2004

silica−alumina showed that the di-cis isomerization on this solid support is selective, indicating that isomerization of Car in a rigid environment is different from that in solvents. In the present study, MCM-41, Ti−MCM-41, and Fe−MCM-41 were chosen as hosts to study the isomerization of Car in the presence of light or by chemical oxidation. MCM-41 is a mesoporous silica containing a regular array of uniform cylindrical pores. The pore size ranges from 15 to 100 Å depending on the chain length of the template used in the synthesis.[14] Previous studies[15−17] have shown that such materials provide an appropriate microenvironment to retard back electron transfer (ET) and thus increase the lifetime of the photoproduced radical ions. MCM-41 with polar −SiOH groups on the surface is a good artificial host for simulation of the protein environment of RCs, although the environment of RCs is much more complicated. Introduction of Ti^{4+} into the MCM-41 framework was found to significantly enhance the photoinduced ET efficiency of Car due to the strong electron-accepting ability of Ti^{4+}.[18] Car embedded in Fe−MCM-41 can be oxidized (without irradiation) to produce $Car^{\bullet+}$. Photolytic isomerization of Car embedded in MCM-41 and Ti−MCM-41 and isomerization of Car embedded in Fe−MCM-41 by chemical oxidation were investigated in this study.

Experimental Section

Synthesis of MCM-41, Ti−MCM-41, and Fe−MCM-41. The procedures used for the preparation of the siliceous material (MCM-41) and Ti−MCM-41 have been previously described.[14,18,19]

According to the literature,[20] ion-exchange was used to synthesize Fe−MCM-41. A mixture of 0.8 g MCM-41 and 30 mL 0.1 M $FeCl_3 \cdot 6H_2O$ ethanolic solution was stirred for 3 h at 60 °C and then filtered. The solid was washed with water in order to remove any ions adsorbed on the external surface. It was then dried at room temperature, heated in an oven at 100 °C for 24 h, and calcined at 450 °C in air for 2 h. A white solid was produced and is designated Fe−MCM-41.

Chemicals. All-trans β-carotene (**I**) and all-trans canthaxanthin (**II**) were purchased from Fluka. Anhydrous dichloromethane was from Aldrich.

EPR and HPLC Sample Preparation. 100 mg of MCM-41 or Ti−MCM-41 or Fe−MCM-41 was activated at 200 °C for 6 h, then at once transferred to a N_2 drybox and allowed to cool to room temperature. 4 mL of 5 mM carotenoid CH_2Cl_2 solution was prepared and added in the drybox; the carotenoid was allowed to diffuse into the molecular sieves for 10 min; the mixture was stirred to evaporate the solvent, and the residue was transferred to an EPR tube, which was then stoppered. The EPR tube was taken out of the drybox, and residual solvent was removed under vacuum (0.01 Torr).

HPLC samples were obtained by extraction of Car with CH_2Cl_2 from the above samples after photoirradiation or oxidation.

Instrumentation. X-ray powder diffraction (XRD) data were obtained from thin layers of samples, and measurements were carried out with a Philips 1840 diffractometer using Cu Kα radiation ($\lambda = 1.541$ Å) within the scattering angle 2θ range of 1.5−10°.

A S-2500 Hitachi scanning electron microscope (SEM) equipped with a Tracor Northern energy dispersive X-ray analysis unit was used to measure the concentrations of Ti^{4+} and Fe^{3+} in Ti−MCM-41 and Fe−MCM-41. The X-ray energy used in the measurements was 15 KV.

A Vydac 201 TP54 polymeric C_{18} column (250 × 4.6 mm i.d.) packed with 5 μm particles (Hesperia, CA) and a Shimadzu LC-600 pump with a SPD-M10AVP PDA detector were used for the HPLC separation and detection. Acetonitrile was the mobile phase. The flow rate of the mobile phase was 1 mL/min.

EPR measurements were carried out with an X-band (9.5 GHz) Varian (Palo Alto, CA) E-12 EPR spectrometer, equipped with a rectangular cavity. The magnetic field was measured with a Bruker (Billerica, MA) EPR 035M gaussmeter, and the microwave frequency was measured with a model HP 5245L frequency counter.

A 250 W xenon lamp (ILC Technology) at a distance of 20 cm was used to irradiate the samples. An optical filter was used to cut off most of the UV light below 350 nm.

AM1 and MM+ (molecular mechanics) calculations were carried out using Hyperchem 6.03 software on a Dell computer (Pentium III). The structures of carotenoid isomers were optimized by AM1 calculations. These structures were used in a MM+ calculation of a cylindrical arrangement of Si−O bonds containing the optimized carotenoid isomer structures.

Results and Discussion

Characteristics of Solid Support Systems MCM-41, Ti−MCM-41, and Fe−MCM-41. The XRD patterns of siliceous MCM-41 molecular sieves after calcination were reported before.[17] Recent more accurate measurements by combined XRD/adsorption analysis showed that the pore size of calcined MCM-41 by a template of micellar surfactant with C_{16} chain length (used in this study) is about 38 Å.[21] Carotenoid molecules (the chain length is about 25 Å) can readily diffuse into such large pores.

Ti−MCM-41 and Fe−MCM-41 showed the same XRD pattern, indicating that the substitution of Ti^{4+} and Fe^{3+} into the framework of MCM-41 does not damage the structure of MCM-41. The Ti/Si atomic ratio of the Ti−MCM-41 sample and the Fe/Si atomic ratio of Fe−MCM-41 were measured by a scanning electron microscope with an energy-dispersive X-ray analysis unit. The ratio is about 0.04 for Ti/Si and 0.03 for Fe/Si. A previous study[22] has shown that these concentrations are suitable for the study of ET for Car embedded in metal ion substituted MCM-41.

Photoisomerization of Car Embedded in MCM-41 and Ti−MCM-41. Figure 1a shows the HPLC of **I**. Figure 1b and c shows the HPLC after 10 min photoirradiation of **I** embedded in MCM-41 and Ti−MCM-41, respectively. The peak assignment is according to previous results.[8−10] ^{1}H NMR spectroscopy and values of the Q ratio[23] (absorbance of the "cis peak"/absorbance of the most intense maximum) were used to identify the isomers. The cis/trans ratios are shown in Table 1. Data[9] of 10 min photoirridiation of **I** in CH_2Cl_2 are also included. Results, summarized in Table 1, clearly demonstrate a strong selectivity for 13-cis formation of **I** embedded in these solid hosts compared to that in CH_2Cl_2. The presence of Ti^{4+} also affects the isomerization. The 9-cis isomer was not formed in MCM-41, but a small amount was also formed in Ti−MCM-41. These results can be attributed to complex formation[18] of Ti^{4+} with **I**. The isomerization efficiency is much higher in these solid hosts than in CH_2Cl_2. To examine whether the selectivity of isomerization in these solid hosts is due to the pore structure of these hosts, **I** was embedded in MCM-41 without removal of the template and the above experiment was repeated. The ratio of 9-cis to 13-cis isomers in this experiment is about 0.5, indicating that the pore structure of MCM-41 causes the selectivity of isomerization. This conclusion is also supported by the following. The 9-cis isomer was not detected by HPLC when the ratio

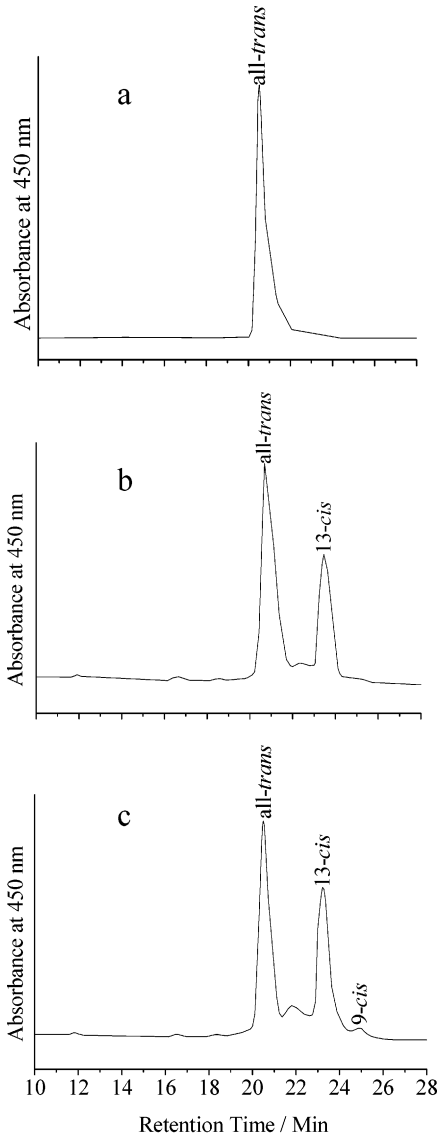

Figure 1. HPLC of **I** (a) and after 10 min photoirradiation of **I** embedded in (b) MCM-41 and (c) Ti−MCM-41.

of **I** to calcined MCM-41 is less than 0.0002 mol/g. If the ratio is greater than 0.0002 mol/g, the ratio of 9-cis to 13-cis increases with the ratio of **I** to MCM-41. These experiments show that the saturation concentration of carotenoid in the pore of MCM-41 is about 0.0002 mol/g.

Figure 2a shows the HPLC of **II**. Figure 2b and c shows the HPLC after 10 min photoirradiation of **II** embedded in MCM-41 and Ti−MCM-41, respectively. The isomers were identified as above. The cis/trans ratios are shown in Table 2. The cis/trans ratios[9] obtained by 10 min photoirradiation of **II** in CH_2Cl_2 are also included. 15-cis and 9,13-di-cis isomers were not detected in the photoirradiation of **II** in CH_2Cl_2, and 15-cis was not detected in the photoirradiation of **II** embedded in MCM-41. Although the isomerization efficiency of **II** embedded in these solid hosts is much higher than that in CH_2Cl_2, the intensity ratios of 9-cis to 13-cis are similar in the three cases, indicating that the solid hosts do not affect the selectivity of isomerization of **II**.

Figure 3a shows the sum of the cis/trans ratios of **I** after 4, 6, 8, and 10 min photoirradiation of **I** embedded in MCM-41 and Ti−MCM-41. Figure 3b shows those for **II**. The isomerization efficiency increases with irradiation time, but the increase decreases with irradiation time, so that there should be limiting values for these cis/trans ratios. The isomerization efficiency is higher for Car embedded in Ti−MCM-41 than in MCM-41.

Whether the isomerization proceeds via the T_1 state of Car or via $Car^{\bullet+}$ was determined by EPR and HPLC measurements as follows. The ratio of intensity of $Car^{\bullet+}$ produced in Ti−MCM-41 to that in MCM-41 after different photoirradiation times at 77 K was compared with the isomerization efficiency (IE) ratio (sum of the cis/trans ratios in Ti−MCM-41 divided by the sum of the cis/trans ratios in MCM-41). Experiment conditions, including the amounts of carotenoids and molecular sieves, were the same in all the measurements. The two ratios for **I** are 3.8 (± 0.6) and 3.0 (± 0.4), respectively, and those for **II** are 3.1 (± 0.6) and 3.3 (± 0.4), respectively. Because the two ratios are comparable within the measurement error range, the isomerization involves $Car^{\bullet+}$. A proposed mechanism is shown below:

$$\textit{trans}\text{-Car} - e \rightleftharpoons \textit{trans}\text{-Car}^{\bullet+}$$

$$\textit{trans}\text{-Car}^{\bullet+} \rightleftharpoons \textit{cis}\text{-Car}^{\bullet+}$$

$$\textit{cis}\text{-Car}^{\bullet+} + e \rightleftharpoons \textit{cis}\text{-Car}$$

A recent study[18] showed that the dication (Car^{2+}) of **I** can also be produced by photoirradiation of **I** in MCM-41 and Ti−MCM-41 because the second oxidation potential of **I** is lower than the first. The singlet Car^{2+}(**I**) was detected optically.[18] For isomerization of **I**, an additional mechanism is proposed as below:

$$\textit{trans}\text{-Car}^{2+}(\mathbf{I}) \rightleftharpoons \textit{cis}\text{-Car}^{2+}(\mathbf{I})$$

$$\textit{cis}\text{-Car}^{2+}(\mathbf{I}) + 2e \rightleftharpoons \textit{cis}\text{-Car}(\mathbf{I})$$

According to a previous study,[8] the isomerization in CH_2Cl_2 also occurs via $Car^{\bullet+}$. The much lower isomerization efficiency in CH_2Cl_2 may be attributed to the much lower electron transfer (ET) efficiency of Car in CH_2Cl_2.

Isomerization of Car in Fe−MCM-41. Figure 4 shows the 77 K EPR spectra of Fe−MCM-41 in the absence and presence of **I**. The signal with *g* value about 4.3 in the EPR spectrum of Fe−MCM-41 is due to Fe^{3+} in an environment of a tetrahedral symmetry,[20] and the broad signal with *g* value about 2.0 is due to Fe^{3+} ions in an environment of octahedral symmetry.[24] The signal with *g* value about 4.3 decreased after **I** was embedded in Fe−MCM-41, and a new signal with *g* value 2.0028 and line width 14.6 G appeared. This new signal is typical for $Car^{\bullet+}$ of **I** on solid support,[25−27] indicating that **I** is oxidized by the tetrahedral Fe^{3+}. Similar results were found for **II** embedded in Fe−MCM-41. This is in contrast to the photoinduced electron transfer of a dicyano-substituted carotenoid in Fe−MCM-41 where the electron is transferred from the carotenoid to the octahedral Fe^{3+}.[28] The fact that the signal with $g = 2.0$ also increases after **I** was embedded in Fe−MCM-41 can be attributed to interaction between Fe^{3+} and **I** (and thus increase the number of octahedral coordination sites). In connection with this, a recent study[22] showed that the interaction between **I** and Cu^{2+} in Cu−MCM-41 can change the Cu^{2+} geometry from orthorhombic to tetragonally square pyramidal coordination. The HPLC is similar to that after 10 min photoirradiation of Car embedded in Ti−MCM-41 (Tables 1 and 2), except that the isomer (**I**) ratio of 9-cis to 13-cis in Fe−MCM-41 is higher than that in Ti−MCM-41 and in Fe−MCM-41 the 15-cis isomer (**I**) is also detected. The high trans-to-cis isomerization efficiency of Car by oxidation with Fe−MCM-41 supports the previous conclusion that the high photoisomerization efficiency of Car

TABLE 1: Approximate cis/trans Ratios of β-Carotene by HPLC Measurements in Different Media and Using Different Methods

	cis/trans ratio (±0.01)					
method	photoirradiation			oxidation	iodine catalysis	electrolysis
medium	CH_2Cl_2[a]	MCM-41	Ti−MCM-41	Fe−MCM-41	hexane[b]	CH_2Cl_2[c]
9-cis	0.05	0	0.03	0.14	0.46	0.36
13-cis	0.04	0.51	0.64	0.70	0.35	0.41
15-cis	0.03	0	0	0.02	0.03	0.04

[a] Reference 9. [b] Reference 11. [c] Reference 8.

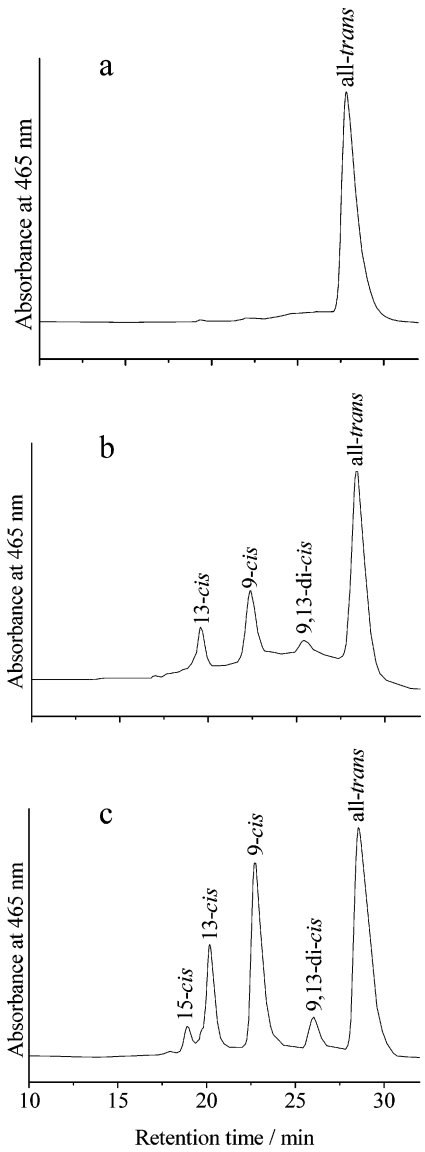

Figure 2. HPLC of **II** (a) and after 10 min photoirrdiation of **II** embedded in (b) MCM-41 and (c) Ti−MCM-41.

embedded in MCM-41 and Ti−MCM-41 is primarily due to the intermediacy of $Car^{\bullet+}$, not the T_1 state of Car. The strongly preferred formation of the 13-cis isomer after oxidation of **I** shows that Fe−MCM-41 also controls the selectivity of isomerization. This is in contrast to the isomerization of **I** by electrolysis of **I** in CH_2Cl_2[8] or by iodine catalysis in hexane[11] (Table 1), which shows that the yield of 13-cis is comparable to that of 9-cis, and that a small amount of the 15-cis isomer is also produced. The fact that the isomer ratio of 9-cis to 13-cis in Fe−MCM-41 is higher than that in MCM-41 and Ti−MCM-41 may be explained as follows: when **I** is added into Fe−MCM-41, some carotenoid may be oxidized by Fe^{3+} outside the pores before diffusing into the pore. For the isomers of **II** produced in Fe−MCM-41, the ratio among the cis isomers is similar to that by electrolysis of **II** in CH_2Cl_2, but it is different from that induced by HCl in CH_2Cl_2 (Table 2). The difference can be attributed to different mechanisms of isomerization. Isomerization in the first two cases proceeds via $Car^{\bullet+}$, that in the third case via $CarH^+$.[12] The isomers produced by oxidation of **II** on silica−alumina are very different from other cases, indicating that the rigid environment of silica−alumina can control the selectivity of the isomerization of **II**.

A possible mechanism for the isomerization of Car in Fe−MCM-41 is shown below:

$$\textit{trans}\text{-Car} + Fe^{3+} \rightleftharpoons \textit{trans}\text{-Car}^{\bullet+} + Fe^{2+}$$

$$\textit{trans}\text{-Car}^{\bullet+} \rightleftharpoons \textit{cis}\text{-Car}^{\bullet+}$$

$$\textit{cis}\text{-Car}^{\bullet+} + \textit{trans}\text{-Car} \rightleftharpoons \textit{cis}\text{-Car} + \textit{trans}\text{-Car}^{\bullet+}$$

$$\textit{cis}\text{-Car}^{\bullet+} + Fe^{2+} \rightleftharpoons \textit{cis}\text{-Car} + Fe^{3+}$$

The last equilibrium is supported by our recent study,[29] which shows that the oxidation of Car with $FeCl_3$ in CH_2Cl_2 is an equilibrium and that $Car^{\bullet+}$ can abstract an electron from Fe^{2+}.

Orientation of I and II in MCM-41 from ENDOR Studies. The orientation of $Car^{\bullet+}$ on solid supports can be studied by ENDOR.[17,27] The ENDOR features of methyl proton couplings are suppressed when methyl groups are close to the surface due to the large anisotropy of these protons (line broadening from incomplete averaging of the methyl proton couplings). The orientations of **I** and **II** in MCM-41 and Ti−MCM-41 have been investigated by optical and ENDOR studies.[18] For **I** embedded in Ti−MCM-41, the maximum absorption wavelength (λ_{max}) of **I** shows a significant 60 nm blue shift compared with that in MCM-41, but this was not observed for **II**. The blue shift for **I** is attributed to the interaction between **I** and Ti^{4+}.[18] These observations suggest that the location of **I** and **II** in these hosts differ. ENDOR studies[18] of $Car^{\bullet+}$(**I**) and $Car^{\bullet+}$(**II**) in Ti−MCM-41 support this suggestion. The ENDOR spectrum of $Car^{\bullet+}$(**I**) does not display the individual peaks expected for couplings of the methyl protons, indicating that the chain of **I** is close and parallel to the surface of the Ti−MCM-41 channel. Since in the ENDOR spectrum of $Car^{\bullet+}$(**II**) in Ti−MCM-41 peaks due to the couplings of C (5 and 5′), C (9 and 9′), and C (13 and 13′) CH_3 protons are detected, the conjugated chain of **II** is located away from the surface of the pore. A simple explanation is that **II** is not encapsulated in the nanoporous channel of MCM-41. If **II** were encapsulated, interaction(s) between the surface of the channel and the methyl groups would result in anisotropic proton hyperfine couplings of methyl group protons. This would appear as broadening of the ENDOR line caused by incomplete averaging of the methyl proton coupling, as is observed for $Car^{\bullet+}$(**I**). The location of **II** is probably at the entrance of the channel (Scheme 2). Because the chain of **II** is distal from the surface of the pore, it can rotate freely, and thus

TABLE 2: Approximate cis/trans Ratios of Canthaxanthin by HPLC Measurements in Different Media and Using Different Methods

	cis/*trans* ratio (±0.01)						
method	photoirradiation			oxidation	electrolysis	HCl catalysis	oxidation
medium	CH_2Cl_2[a]	MCM-41	Ti−MCM-41	Fe−MCM-41	CH_2Cl_2[b]	CH_2Cl_2[c]	silica−alumina[d]
9-cis	0.07	0.22	0.55	0.58	0.35	0.24	
13-cis	0.03	0.11	0.24	0.25	0.19	0.22	
15-cis	0	0	0.02	0.03	0.02	0	
9,13-di-cis	0	0.03	0.07	0.08	0.04	0	
13,13′-di-cis	0	0	0	0	0	0.04	
11,11′-di-cis	0	0	0	0	0	0	*d*
11,15-di-cis	0	0	0	0	0	0	*d*

[a] Reference 9. [b] Reference 8. [c] Reference 12. [d] Reference 13, no HPLC measurements carried out. Detected 11,11′-di-cis and 11,15-di-cis in addition to the all trans form by HYSCORE, pulsed EPR techniques. It is not certain from pulsed measurements whether other cis isomers occur.

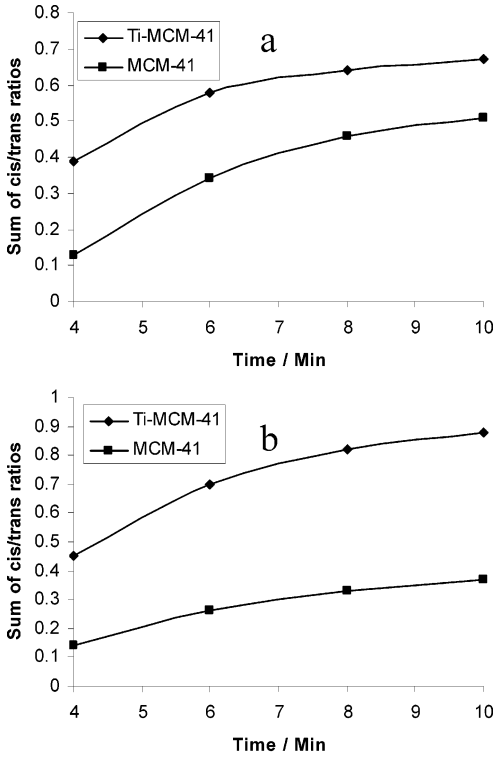

Figure 3. Sum of the cis/trans ratios after 4, 6, 8, and 10 min photoirradiation of (a) **I** and (b) **II** embedded in MCM-41 and Ti−MCM-41.

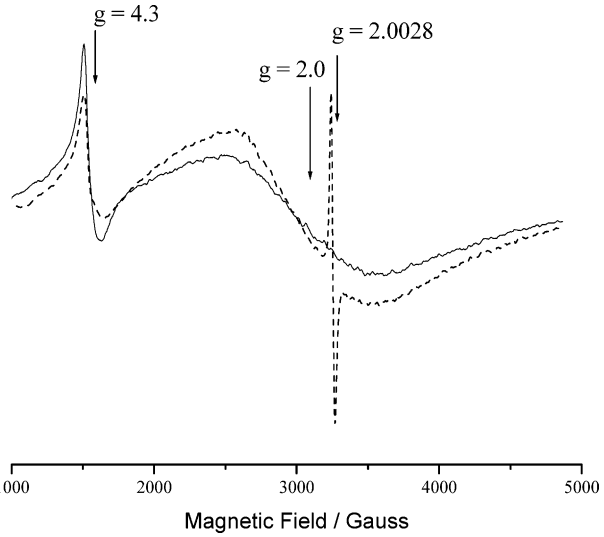

Figure 4. 77 K EPR spectrum of Fe−MCM-41 (solid line) and after **I** was embedded in Fe−MCM-41 (dashed line).

SCHEME 2. Location of II in MCM-41

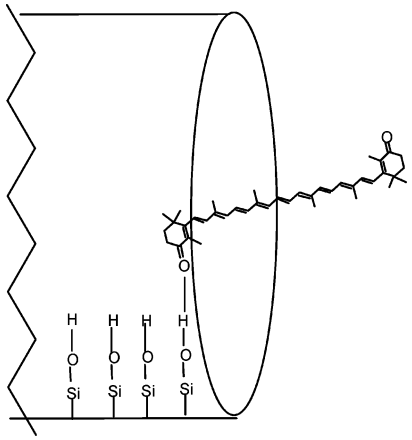

the relative amounts of the cis isomers are similar to those observed for the cis isomers formed in solvents. The difference in the location of these two compounds can be attributed to the difference in the terminal functionalities. The oxygen atoms in the cyclohexene rings of **II** may H-bond to the −SiOH groups on the external surface or at the entrance. The strong selective isomerization of **II** on silica−alumina can be attributed to the fact that the orientation of **II** on the surface of silica−alumina is different from that in MCM-41 (for **II** on the silica−alumina surface, the middle of the chain of **II** interacts with the surface.[13,27]).

Molecular Mechanics Calculation. The strong selectivity for formation of the 13-cis isomer of **I** in the channels of MCM-41 may be attributed to the shape of the channel, which allows sufficient interaction of the 13-cis isomer and the surface of the pore so that the system energy is lower than that with other cis isomers. Since the isomers are encapsulated in the nanoporous cylindrical channel of MCM-41, the simplest way to simulate this confinement is to place the isomers in a cylinder[19] of Si−O bonds with the same diameter as that of the pores (38 Å), although a more accurate and efficient method to study the adsorption of molecules in MCM-41 models, which were built using Monte Carlo simulations, was developed recently.[30] Figure 5 shows the minimum energy location of the cis isomers in a cylindrical arrangement of Si−O bonds. The geometry of the cis carotenoid isomer was optimized by the AM1-RHF method. Because the system contains about 1000 atoms, the molecular mechanics force field MM+ method available in the Hyperchem (version 6.03) program was used to calculate the system energy (other semiempirical calculation methods could not be used to calculate the system energy because these require more than the available memory of the computer). MM+ is the simplest

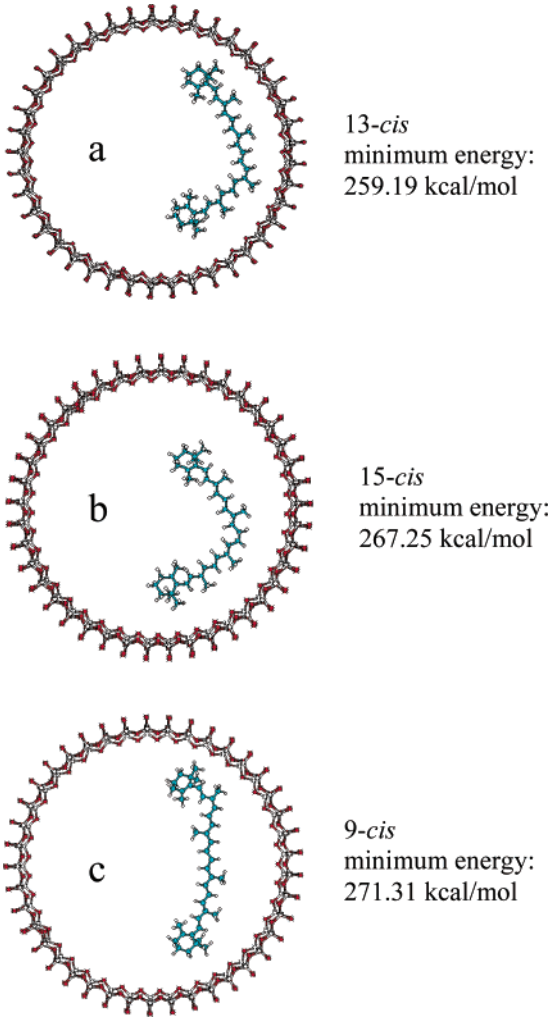

Figure 5. Minimum energy location of isomers of **I** (a) 13-cis, (b) 15-cis, and (c) 9-cis in a cylindrical arrangement of Si−O bonds.

of the molecular mechanic calculation methods and the Lennard-Jone interatomic potential was used to simulate van der Waals interaction. The MM+ program ignores atomic charges and uses dipole moments supplied in its parameter set. In our calculations, the electrostatic interactions were calculated using the bond dipole interaction option. The bond dipole values come from the MM+ stretch parameter file provided in the Hyperchem program. The cutoffs option is "None", which means that all nonbonded interactions are calculated for systems in vacuo. No periodical boxes or boundary conditions were used. The Polak−Ribiere conjugated gradient method was used. This method uses one-dimensional searches and considers the previous conjugated direction. This method converges more quickly than the Fletcher−Reeves method but needs slightly more memory. The RMS energy minimization gradient was set equal to 0.01 kcal/Å mol. To obtain the minimum energy location for every isomer, dozens of orientations of the carotenoid isomers in the cylinder were calculated and compared. The calculations showed that when the minimum energy is achieved, the closest distance between the chain of a carotenoid isomer and the wall of the cylinder is ~5 Å. The minimum energies for the system with 13-cis, 9-cis, and 15-cis isomers are 259.19, 271.31, and 267.25 kcal/mol, respectively. The 13-cis conformation results in the lowest system energy, in agreement with preferred formation of this isomer. Calculations for di-cis isomers were not carried out because these were not detected.

Conclusions

High isomerization efficiency of Car embedded in MCM-41 or in metal ion substituted MCM-41 can be obtained by photoexcitation or oxidation. The isomerization occurs primarily via $Car^{\bullet+}$. The environment in MCM-41 pores causes a selectivity of isomerization for Car whose framework is close to the surface of these solid hosts. This is in contrast to the isomerization in solvent by photoexcitation, iodine or acid catalysis, acid-induction, and electrolysis, and this is also different from the isomerization on silica−alumina. The presence of transition metal ions also affects the isomerization. This study contributes to our understanding of the isomerization behavior of carotenoids in photosystem II and points to potential applications in catalysis. Further work should ascertain how different pore sizes and different functional groups on the surface of the pores affect the selectivity.

Acknowledgment. Dr. Langqiu Xu (Argonne National Laboratory) and the late Dr. Larry Kevan (Chemistry Department, University of Houston) are thanked for suggestions for synthesizing MCM-41 and Ti-MCM-41. Ms. Jolanta Nunley (Biological Sciences Department, University of Alabama) is thanked for the SEM measurement. Dr. Rainer Schad is thanked for the XRD measurements. Dr. Elli Hand is thanked for helpful discussions. This work was supported by the Chemical Sciences, Geosciences and Biosciences Division, Office of Basic Energy Sciences, Office of Science, U.S. Department of Energy under Grant No. DE-FG02-86ER 13465.

References and Notes

(1) Frank, H. A.; Young, A. J.; Britton, G.; Cogdell, R. J. *The Photochemistry of Carotenoids*, Kluwer: The Netherlands, 1999; pp 161−188.
(2) Kuki, M.; Koyama, Y.; Nagae, H. *J. Phys. Chem.* **1991**, *95*, 7171.
(3) Bialek-Bylka, G. E.; Tomo, T.; Satoh, K.; Koyama, Y. *FEBS Lett.* **1995**, *363*, 137.
(4) Mathis, P.; Rutherford, A. *Biochim. Biophys. Acta* **1984**, *767*, 217.
(5) De Las Rivas, J. O.; Telfer, A.; Barber, J. *Biochim. Biophys. Acta* **1993**, *1142*, 155.
(6) Piekara-Sady, L.; Jeevarajan, A. S.; Kispert, L. D. *Chem. Phys. Lett.* **1993**, *207*, 173.
(7) Hanley, J.; Deligiannakis, Y.; Pascal, A.; Faller, P.; Rutherford, A. W. *Biochem.* **1999**, *38*, 8195.
(8) Gao, G.; Wei, C. C.; Jeevarajan, A. S.; Kispert, L. D. *J. Phys. Chem.* **1996**, *100*, 5362.
(9) Gao, G.; Deng, Y.; Kispert, L. D. *J. Phys. Chem. B* **1998**, *102*, 3897.
(10) Wei, C. C.; Gao, G.; Kispert, L. D. *J. Chem. Soc., Perkin Trans. 2* **1997**, 783.
(11) Emenhiser, C.; Sander, L. C.; Schwartz, S. J. *J. Chromato. A* **1995**, *707*, 205.
(12) Konovalov, V. V.; Kispert, L. D. *J. Chem. Soc., Perkin Trans. 2* **1999**, 901.
(13) Konovalova, T. A.; Dikanov, S. A.; Bowman, M. K.; Kispert, L. D. *J. Phys. Chem. B* **2001**, *105*, 8361.
(14) Beck, J. S.; Vartuli, J. C.; Roth, W. J.; Leonowicz, M. E.; Kresge, C. T.; Schmit, K. D.; Chu, T.-W.; Olson, D. H.; Shepperd, E. W.; McCullen, S. B.; Higgins, J. B.; Schlenker, J. L. *J. Am. Chem. Soc.* **1992**, *114*, 10834.
(15) Krishna, R. M.; Prakash, A. M.; Kevan, L. *J. Phys. Chem. B* **2000**, *104*, 1796.
(16) Sung-Suh, H. M.; Luan, Z.; Kevan, L. *J. Phys. Chem. B* **1997**, *101*, 10455.
(17) Konovalova, T. K.; Gao, Y.; Schad, R.; Kispert, L. D.; Saylor, C. A.; Brunel, L.-C. *J. Phys. Chem. B* **2001**, *105*, 7459.
(18) Gao, Y.; Konovalova, T. A.; Xu, T.; Kispert, L. D. *J. Phys. Chem. B* **2002**, *106*, 10808.
(19) Maschmeyer, T.; Rey, F.; Sankar, G.; Thomas, J. M. *Nature* **1995**, *378*, 159.
(20) Bourlinos, A. B.; Karakassides, M. A.; Petridis, D. *J. Phys. Chem. B* **2000**, *104*, 4375.

(21) Kruk, M.; Jaroniec, M.; Sakamoto, Y.; Terasaki, O.; Ryoo, R.; Ko, C. H. *J. Phys. Chem. B* **2000**, *104*, 292.
(22) Gao, Y.; Konovalova, T. A.; Lawrence, J. N.; Smitha, M. A.; Nunley, J.; Schad, R.; Kispert, L. D. *J. Phys. Chem. B* **2003**, *107*, 2459.
(23) Dewar, M. J. S.; Zoebisch, E. G.; Healy, E. F.; Stewart, J. J. P. *J. Am. Chem. Soc.* **1985**, *107*, 3902.
(24) (a) Mansanares, A. M.; Baesso, M. L.; da Silva, E. C.; Gandra, F. C. G.; Vargas, H.; Mirtanda, L. C. M. *Phys. Rev. B* **1989**, *40*, 7912. (b) Goldfarb, D.; Bernardo, M.; Strohmaier, K. G.; Vaughan, D. E. W.; Thomann, H. *J. Am. Chem. Soc.* **1994**, *116*, 6344. (c) Manhães, R. S. T.; Auler, L. T.; Sthel, M. S.; Alexandra, J.; Massunaga, M. S. O.; Carrió, J. G.; dos Santos, D. R.; da Silva, E. C.; Garcia-Quiroz, A.; Vargas, H. *Appl. Clay Sci.* **2002**, *21*, 303.
(25) Jeevarajan, A. S.; Khaled, M.; Kispert, L. D. *J. Phys. Chem.* **1994**, *98*, 7777.
(26) Jeevarajan, A. S.; Khaled, M.; Kispert, L. D. *Chem. Phys. Lett.* **1994**, *225*, 340.
(27) Jeevaranjan, A. S.; Kispert, L. D.; Piekara-Sady, L. *Chem. Phys. Lett.* **1993**, *209*, 269.
(28) Konovalova, T. A.; Gao, Y.; Kispert, L. D.; van Tol, J.; Brunel, L.-C. *J. Phys. Chem. B* **2003**, *107*, 1006.
(29) Gao, Y.; Kispert, L. D. *J. Phys. Chem. B* **2003**, *107*, 5333.
(30) He, Y.; Seaton, N. A. *Langmuir* **2003**, *19*, 10132.